Direct Numerical Simulation of structural vacillation in the transition to geostrophic turbulence

Anthony Randriamampianina, Pierre Maubert, Wolf-Gerrit Früh, Peter L. Read

▶ **To cite this version:**

Anthony Randriamampianina, Pierre Maubert, Wolf-Gerrit Früh, Peter L. Read. Direct Numerical Simulation of structural vacillation in the transition to geostrophic turbulence. Congrès Français de Mécanique CFM2007, Aug 2007, Grenoble, France. pp.CFM2007-1286. hal-00192614

HAL Id: hal-00192614
https://hal.science/hal-00192614

Submitted on 28 Nov 2007

HAL is a multi-disciplinary open access archive for the deposit and dissemination of scientific research documents, whether they are published or not. The documents may come from teaching and research institutions in France or abroad, or from public or private research centers.

L'archive ouverte pluridisciplinaire **HAL**, est destinée au dépôt et à la diffusion de documents scientifiques de niveau recherche, publiés ou non, émanant des établissements d'enseignement et de recherche français ou étrangers, des laboratoires publics ou privés.

Direct Numerical Simulation of structural vacillation in the transition to geostrophic turbulence

Anthony Randriamampianina[1], **Pierre Maubert**[1], **Wolf G. Früh**[2] **& Peter L. Read**[3]

[1] *Institut de Recherche sur les Phénomènes Hors Equilibre, UMR 6594 CNRS*
Technopôle de Château-Gombert. 49, rue Frédéric Joliot-Curie. BP 146
13384 Marseille cedex France
[2] *School of Engineering and Physical Sciences, Heriot Watt University*
Riccarton, Edinburgh, EH14 4AS, UK
[3] *Atmospheric, Oceanic and Planetary Physics*
University of Oxford, Department of Physics
Clarendon Laboratory, Parks Road, Oxford, OX1 3PU, UK
Corresponding author: randria@irphe.univ-mrs.fr

hal-00192614, version 1 - 28 Nov 2007

Abstract :

The onset of small-scale fluctuations around a steady convection pattern in a rotating baroclinic annulus filled with air is investigated using Direct Numerical Simulation. In previous laboratory experiments of baroclinic waves, such fluctuations have been associated with a flow regime termed Structural Vacillation which is regarded as the first step in the transition to fully-developed geostrophic turbulence.

Résumé :

Le développement de fluctuations de petite échelle dans un écoulement convectif permanent d'air en cavité tournante barocline est analysé par simulation numérique directe. Des travaux expérimentaux antérieurs ont associé de telles fluctuations au régime de vacillation structurelle, considéré comme la première étape vers la turbulence géostrophique.

Key-words :

Structural Vacillation ; Barotropic instability ; Geostrophic turbulence

1 Introduction

The transition to disordered behaviour in the form of 'Baroclinic Chaos' provides an important prototypical form of chaotic transition in fluid dynamics. This is of particular geophysical relevance in the context of understanding the origins of chaotic behaviour and limited predictability in the large-scale atmospheres of the Earth and other terrestrial planets, such as Mars, and in the oceans (e.g Pierrehumbert & Swanson (1995); Read *et al*. (1998); Read (2001)). For many years, the differentially-heated, rotating cylindrical annulus has proved a fruitful means of studying fully-developed, nonlinear baroclinic instability in the laboratory (Fowlis & Hide (1965), Früh & Read (1997)). Transitions within the regular wave regime follow canonical bifurcations to low-dimensional chaos, but disordered flow appears to emerge via a different mechanism involving small-scale secondary instabilities. Not only is the transition to geostrophic turbulence less well understood than those within regular waves, but also the classification and terminology for the weakly turbulent flows is rather vague. Various terms applied include Structural Vacillation or Tilted-Trough Vacillation which both refer to fluctuations by which the wave pattern appears to change its orientation or structure in a roughly periodic fashion. These fluctuations have been explained by the growth of higher order radial mode baroclinic waves (Weng & Barcilon (1987)), by barotropic instabilities, or by small-scale secondary

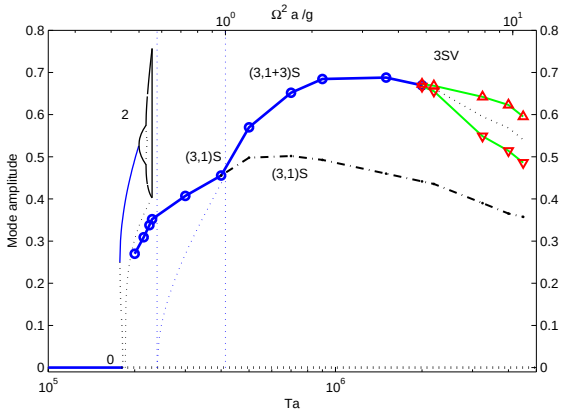

Figure 1: Summary of the regimes obtained by the numerical model for a temperature difference of $\Delta T = 30\mathrm{K}$. The axis at the bottom shows the Taylor number while the axis at the top shows the ratio of the centrifugal term to gravity at the inner radius.

instabilities or eddies, which lead to erratic modulations of the large-scale pattern (Hignett *et al*. (1985)). Subsequent development within this so-called 'transition zone' leads to the gradual and progressive breakdown of the initially regular wave pattern into an increasingly disordered flow, ultimately leading to a form of 'geostrophic turbulence' (Read (2001)).

2 The numerical model

The physical model comprises a body of air contained between two vertical, coaxial cylinders held at constant temperatures and two horizontal insulating rigid endplates separated by a distance of d. The inner cylinder at radius $r = a$ is cooled (T_a) and the outer cylinder at radius $r = b$ is heated ($\Delta T = T_b - T_a = 30K$). The whole cavity rotates at a uniform rate around the axis of the cylinders. The geometry is defined by an aspect ratio, $A = d/(b-a) = 3.94$ and a curvature parameter, $R_c = (b+a)/(b-a) = 3.7$, corresponding to the configuration used by Fowlis & Hide (1965) in their experiments with liquids. Following a long-established tradition (e.g. Fowlis & Hide (1965)), the analysis of the flow in a fixed geometry for a given fluid, here air at ambient temperature with $Pr = 0.707$, is made by varying two main parameters: the Taylor number Ta and the thermal Rossby or 'Hide' number Θ,

$$Ta = \frac{4\Omega^2(b-a)^5}{\nu^2 d}, \quad \Theta = \frac{gd\alpha\Delta T}{\Omega^2(b-a)^2}.$$

The Navier-Stokes equations coupled with the energy equation via the Boussinesq approximation are solved using a pseudo-spectral collocation-Chebyshev Fourier method associated with a second order time scheme.

3 The onset of SV regime

Figure 1 shows the equilibrated amplitude of the dominant azimuthal mode against the Taylor number. For steady solutions, the equilibrated amplitude of that wave mode is shown while for time-dependent solutions, the maximum and minimum as well as the mean amplitude are given. As such, the figure is a bifurcation diagram representing the sequence of three basic solutions, the axisymmetric solution on the x-axis and the $m = 2$ and $m = 3$ solutions pro-

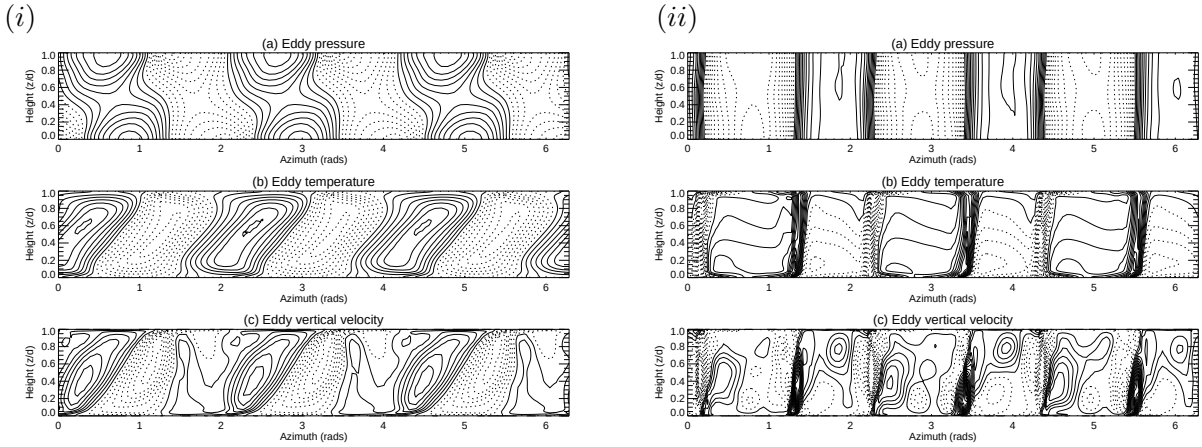

Figure 2: Azimuth-height maps of eddy fields (with azimuthal flow removed) of a wave-3 simulation at (i) $Ta = 0.235 \times 10^6$; (ii) $Ta = 4. \times 10^6$. (a) Pressure (contour interval = 0.25 dimensionless units), (b) Temperature (contour interval = 0.05, normalised to an imposed temperature difference of ± 1.0) and (c) Vertical velocity (contour interval = 0.5 dimensionless units).

jected onto the same plane. The instability of the axisymmetric solution and the $m = 2$ solution branch are reproduced from the earlier study in Randriamampianina *et al*. (2006). The present study focusses on evolution of the $m = 3$ solution branch when increasing progressively the rotation rate up to $Ta = 5. \times 10^6$. A transition in the flow structure is observed, where the three-dimensional structure of the flow responds to a shift in the balance between gravity and the centrifugal force, quantified by the local Froude number, $Fr = \Omega^2 r/g$, and the dominant physical process changes from baroclinic instability to convection due to radial buoyancy. The transition of this convection to chaotic behaviour is fundamentally different from that observed in the transition to the chaotic flow observed at lower rotation rates. Rather than via a sequence of low-dimensional, quasi-periodic states, the large-scale convection developed small-scale instabilities, which have been previously suggested as the origin of Structural Vacillation (SV) within the transition to geostrophic turbulence.

The Froude number taken at the inner radius $Fr_a \equiv \Omega^2 a/g$ was used as the secondary axis on top of the graph in Figure 1 and the location of $Fr_a = 1$ is highlighted by the dotted vertical line at $Ta = 414,000$. The first vertical line, at $Ta = 239,000$, indicates where the centrifugal force equals gravity at the outer cylinder, $Fr_b = 1$. Below that Froude number or Taylor number, gravity is the stronger of the two forces everywhere in the annulus. It can be seen that $Fr_a = 1$ corresponds to a place on the solution branch where the radial structure of the steady wave changes. At the bifurcation, a higher radial mode of the same azimuthal wave grows to a finite amplitude while the first radial mode appears saturated around $Ta \sim 10^6$ and even decays. In terms of the physical quantities, this development results in strong velocity and temperature gradients near the boundaries and the concentration of the radial transport of heat and momentum in narrow plumes or jets. At the highest values of Taylor numbers explored, 2 to 5×10^6, that flow then developed temporal fluctuations.

This change from a regular steady wave dominated by baroclinic instability to the transition zone characterized by small-scale fluctuations can be seen from the variations of eddy variables at two different values of rotation rates in the azimuth-height maps at mid-radius in Figure 2. At $Ta = 0.235 \times 10^6$, the solution shows a pressure field which tilts westward with height and the temperature and vertical velocity fields which tilt eastward in such a way that the strongest upwelling is located around the strongest temperature gradient and strongest pressure gradient

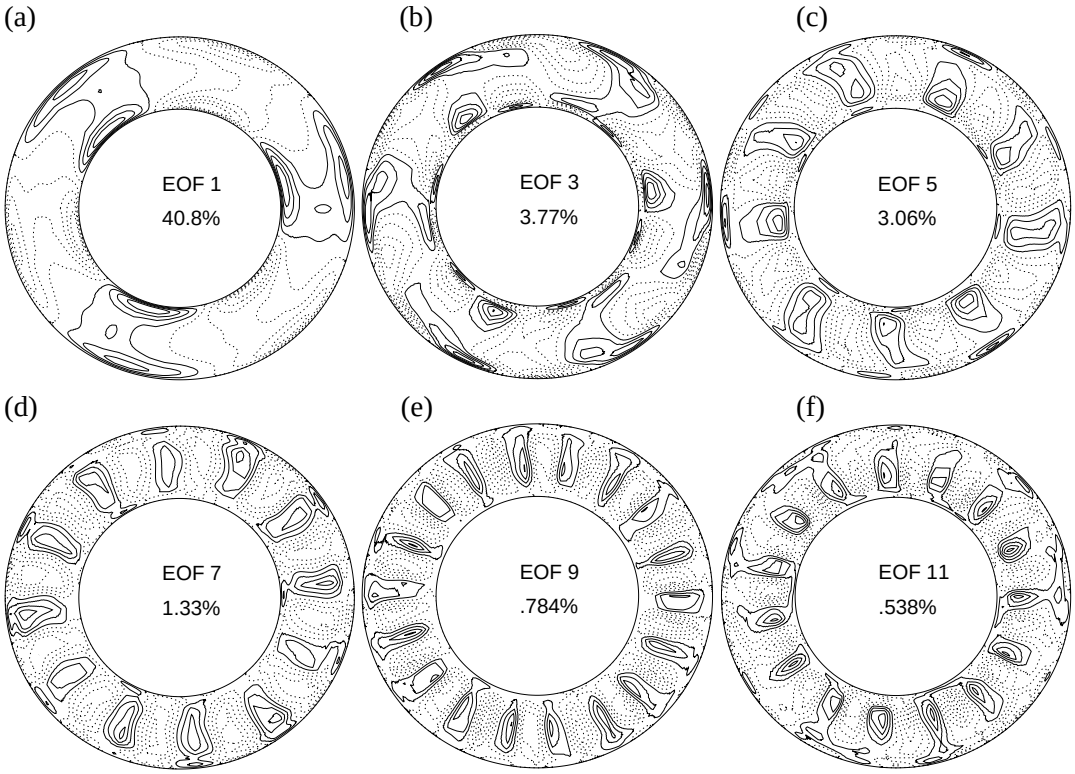

Figure 3: Maps of the odd EOFs of the first six pairs EOFs of temperature at mid-height from a simulation of baroclinic waves in air at Ta = 4.0×10^6. EOFs are shown in order of decreasing contribution to the total temperature variance at this level.

near the lower boundary. This behaviour is that of a typical baroclinic steady wave. At higher rotation rate $Ta = 4. \times 10^6$, the pressure field clearly shows very little phase tilt with height while the temperature field exhibits highly concentrated plumes of hot and cold air which have very little slope with height, interspersed with broad regions with relatively very weak horizontal thermal gradients. The thermal plumes are aligned azimuthally with the regions of strong azimuthal pressure gradient, consistent with optimising the correlation between radial (geostrophic) velocity and temperature perturbations. Similarly, the regions of strong upward vertical velocity are also concentrated close to the strongest positive temperature anomalies, and *vice versa*, consistent with an optimisation of $\overline{w'T'}$ (where w' and T' represent departures in vertical velocity and temperature from their azimuthal mean values). Eventually, the decrease of the tilt results in a virtually vertical, 'barotropic' structure. Regions of strong downward motion (necessary to satisfy mass conservation) are concentrated in plumes or jets adjacent to the strong upwelling jets, forming 'cross-frontal' circulations which show some similarities with those inferred for atmospheric frontal regions in developing cyclones (Hoskins (1982)). The overall impression is that the flow in this region of parameter space is strongly nonlinear and much modified from the simple, linearly unstable Eady solution found at much lower Taylor number.

4 The SV characteristics

The spatial structure associated especially with the onset of structural vacillation is of particular interest, since it may be associated with bifurcations involving quite different spatial modes. As a means of isolating the dominant patterns in the flow, we have made use of a form of Empirical

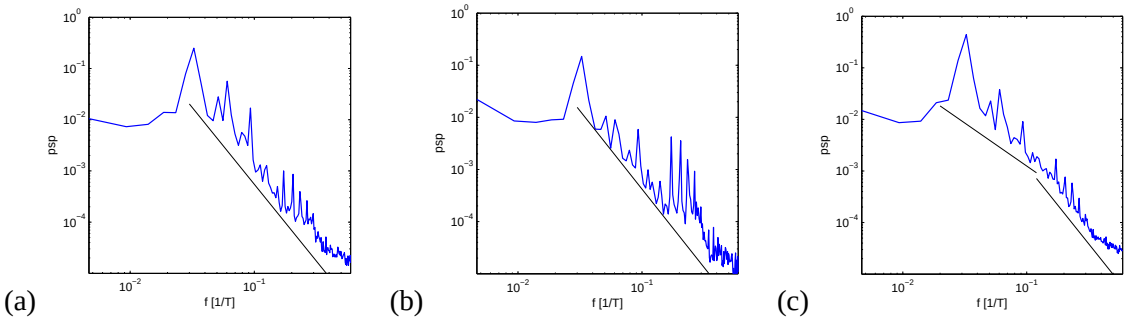

Figure 4: Power spectra from the time series of the temperature after removing the steady wave: (a) near the inner wall, (b) at mid-radius, and (c) near the outer wall. All show a line $\sim f^{-3}$ but (c) also shows a line $\sim f^{-5/3}$ at the lower frequencies.

Orthogonal Function (EOF) analysis (Preisendorfer (1988)), in which time sequences of spatial maps e.g. of temperature were analysed to obtain the covariance matrix of every spatial point with every other in the two-dimensional field.

Figures 3 show the first six pairs of EOFs at $Ta = 4.0 \times 10^6$, which together account for a little over 98% of the temperature variance. However, the first six EOFs appear as three conjugate pairs and represent 93.2% of the variance, indicating a slightly broader spread into the higher order patterns. The first two EOFs, e.g. Fig. 3(a), correspond to pattern dominated by $m = 3$, where the radial structure seems somewhat more concentrated towards the side boundaries, with only weak amplitude throughout most of the interior radii. EOFs 3 and 4, Fig. 3(b), show a pattern dominated by $m = 6$, but with even more contorted phase shifts with radius. The overall impression is of a pattern represented by $m = 6$ in azimuth and $l = 4$ in radius (where l is a nondimensional radial wavenumber). Subsequent EOFs display patterns with a reasonably simple $l = 1$ radial structure (except for (c), which also shows evidence for $l = 4$ dependence on r in EOFs 3 and 4), and increasing azimuthal harmonics of $m = 3$. The higher order EOFs in Figs 3(c) and (d) generally have a much simpler radial structure, with a simple maximum in amplitude near mid-radius and only weak phase-tilts with radius. They again appear in conjugate pairs, and represent other azimuthal harmonics of $m = 3$. The complex phase variations with radius in EOFs 3 and 4 demonstrate the growth of higher radial modes as previously supposed in Figure 1, though the patterns in (c) and (d) of Figs 3 would seem to suggest such anti-correlations ought to be strongest for $m = 6$ rather than the dominant $m = 3$.

Spatially averaged power spectra from the temperature residuals, after removing the steady wave, at mid-height and three radial positions, at mid-radius and around 15% from each wall, are shown in Figure 4. The main frequency ($\sim 0.03T^{-1}$, with the time scale $T = 1/2\Omega$) is that of the emission of the perturbations described by EOFs 3 and 4. The spectrum falls off at all radial positions, with some distinctive peaks over the general decay. While the decay at higher frequencies is largely consistent with a f^{-3} law at all postions, a slight flattening in the frequency range between that of the main perturbation and about $0.1T^{-1}$ can be observed near the outer wall. The behaviour of the spectrum in that range appears to be closer to a $f^{-5/3}$ law.

The spectral evidence suggests that the flow investigated here consists of a fairly steady large-scale convection pattern in the form of three pairs of hot and cold radial jets. From those jets, smaller perturbations are emitted at relatively regular intervals where a jet approaches a wall. The overall flow field responds in a cascade of faster (and presumably smaller) fluctuations which appear consistent with two-dimensional, quasi-geostrophic turbulence over a wide range of frequencies similar to results of DNS of geostrophic turbulence. Recently, similar energy

spectra were observed for geostrophic turbulence in a square box (Lindborg & Alvelius (2000); Waite & Bartello (2006)).

5 Conclusions

In the present work, we find the emergence of a new steady wave solution with complex radial structure, associated with a change in the balance of forces to a centrifugally-dominated regime, followed (at high Taylor number) by a further transition to a form of structural vacillation associated with regular m = 3 eddies driven by centrifugal buoyancy. The computations have been carried out on the NEC SX-5 of the IDRIS (CNRS, Orsay, France). The authors are grateful to the British Council and the CNRS for funding the collaboration between the French and UK partners in a joint programme Alliance.

References

W. W. Fowlis and R. Hide 1965 Thermal convection in a rotating annulus of liquid : effect of viscosity on the transition between axisymmetric and non-axisymmetric flow regimes. *J. Atmos. Sci.* **22** 541-558

W.-G. Früh and P. L. Read 1997 Wave interactions and the transition to chaos of baroclinic waves in a thermally driven rotating annulus. *Phil. Trans. R. Soc. Lond. (A).* **355** 101-153

P. Hignett, A. A. White, R. D. Carter, W. D. N. Jackson and R. M. Small 1985 A comparison of laboratory measurements and numerical simulations of baroclinic wave flows in a rotating cylindrical annulus. *Quart. J. R. Met. Soc.* **111** 131-154

B. J. Hoskins 1982 The mathematical theory of frontogenesis. *Ann. Rev. Fluid Mech.* **14** 131-154

E. Lindborg and K. Alvelius 2000 The kinetic energy spectrum of the two-dimensional enstrophy turbulence cascade. *Phys. Fluids.* **12(5)** 945-947

R. T. Pierrehumbert and K. L. Swanson 1995 Baroclinic instability. *Ann. Rev. Fluid Mech.* **27** 419-467

R. W. Preisendorfer 1988 *Principal Component Analysis in Meteorology and Oceanography.* Elsevier, Amsterdam

A. Randriamampianina, W.-G. Früh, P. Maubert and P. L. Read 2006 Direct Numerical Simulation of bifurcations in an air-filled rotating baroclinic annulus. *J. Fluid Mech.* **561** 359-389

P. L. Read 2001 Transition to geostrophic turbulence in the laboratory, and as a paradigm in atmospheres and oceans. *Surveys in Geophys.* **22** 265-317

P. L. Read and M. Collins and W.-G. Früh and S. R. Lewis and A. F. Lovegrove 1998 Wave interactions and baroclinic chaos: a paradigm for long timescale variability in planetary atmospheres. *Chaos, Solitons & Fractals.* **9** 231-249

M.L. Waite and P. Bartello 2006 The transition from geostrophic to stratified turbulence. *J. Fluid Mech.* **568** 89-108

H.-Y. Weng and A. Barcilon 1987 Wave structure and evolution in baroclinic flow regimes. *Quart. J. R. Met. Soc.* **113** 1271-1294